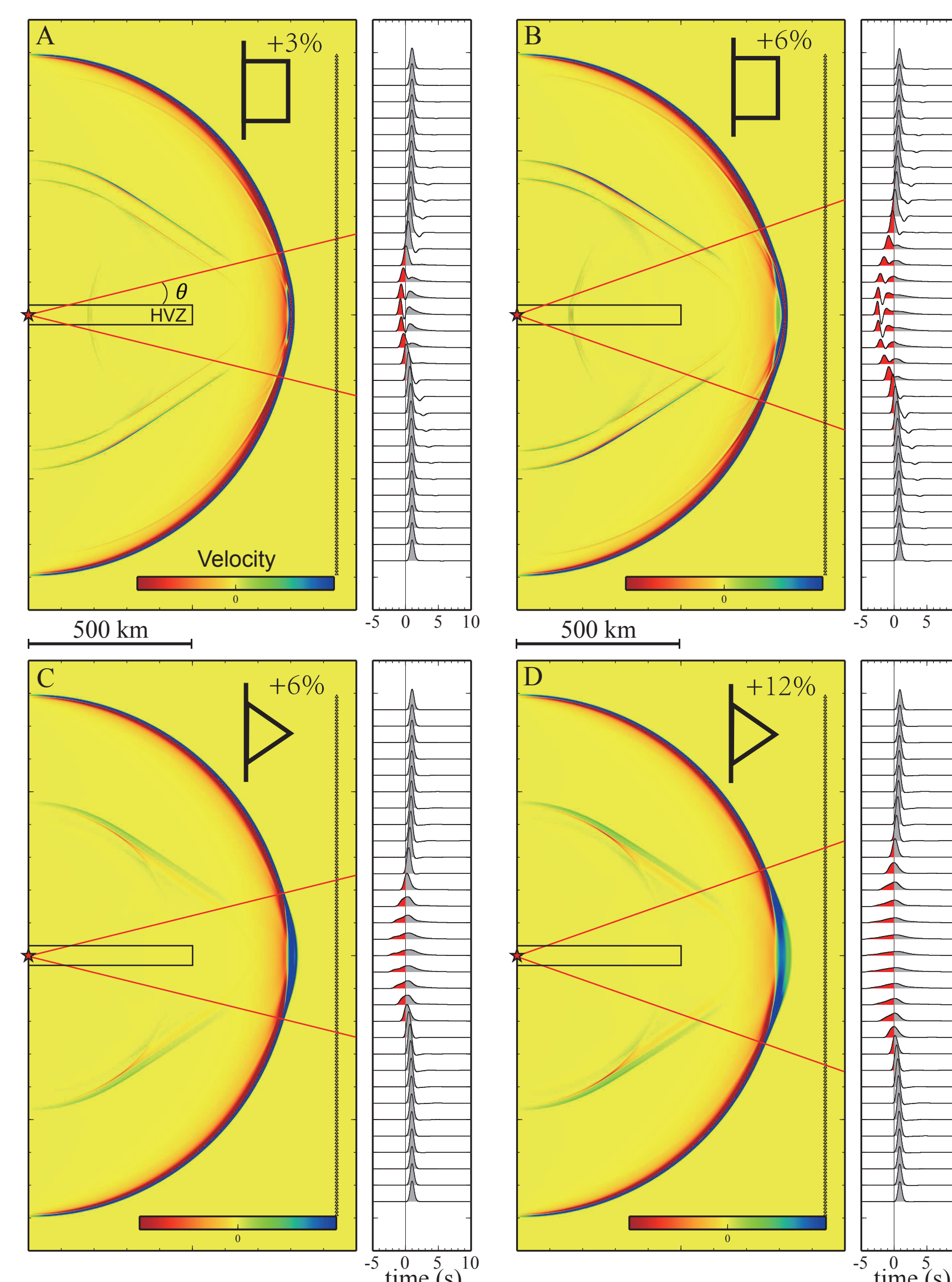


## Abstract

The geometry of subducted slabs are not well imaged in most tomographic models with anomalies typically less than 1%. Synthetics for such models are not noticeably different from their 1D reference model. In contrast, observed teleseismic waveforms sampling slabs in the down-dip direction display multipathing features indicative of substantial structure. Such waveform complexity patterns appear distinctly different for various source locations with outer-rise events, prior to subduction, generally displaying relatively simple waveforms. Here, we model these waveform patterns for a portion of the Kuril subduction zone. The best fitting models have smooth edges with relatively fast cores (>5%) compatible with thermal modeling in shape. Complete seismograms for these 2D models indicate that multibounce P and S waves are slab-sensitive and can be used in refining models.

## Introduction

Seismic images have revealed a complicated fate of subducted slabs, including penetrating into the lower mantle, stagnating in the transition zone, flat subducting and tearing. Approaches to derive these slab images are based mostly on travel times, and have evolved in the last decades with increasing data sets and progress in methodology. However, resolution of tomography is limited by data coverage, damping and accuracy of earthquake locations. For example, in most tomography models, the velocity perturbations of slabs are on the order of 1%, much smaller than the earlier results (~5%) from travel-time modeling mentioned above or waveform modeling discussed in the following.



**Figure 1. Waveform effects of a high-velocity slab.** Examples of waveform complexity caused by a high-velocity slab. The finite-difference simulations of the full wavefield from an explosion source (star) at the left end of various high velocity slabs (black rectangle) are displayed assuming a grid-size of 1 km. In (A), the velocity profile across the slab is uniformly 3% higher than the homogeneous ambient material ( $V_p=8$  km/s) as shown by the inset. The background shows a snapshot of the velocity wavefield with strong P waves and weak P-to-S converted phases from slab edges. The right panel displays the synthetic seismograms recorded on the linear array (small triangles) in the right part of the model. The seismograms are aligned by predicted travel times without the slab, and the earlier arrivals are filled by the red color. The wedge defined by the two red lines displays the range of stations with waveform distortions. (B) Similar to (A) but with a 6% uniform velocity perturbation within the slab. (C) Similar to (A) but with triangular velocity profile across the slab as shown by the inset. (D) Similar to (C) but with a 12% velocity perturbation in the slab core.

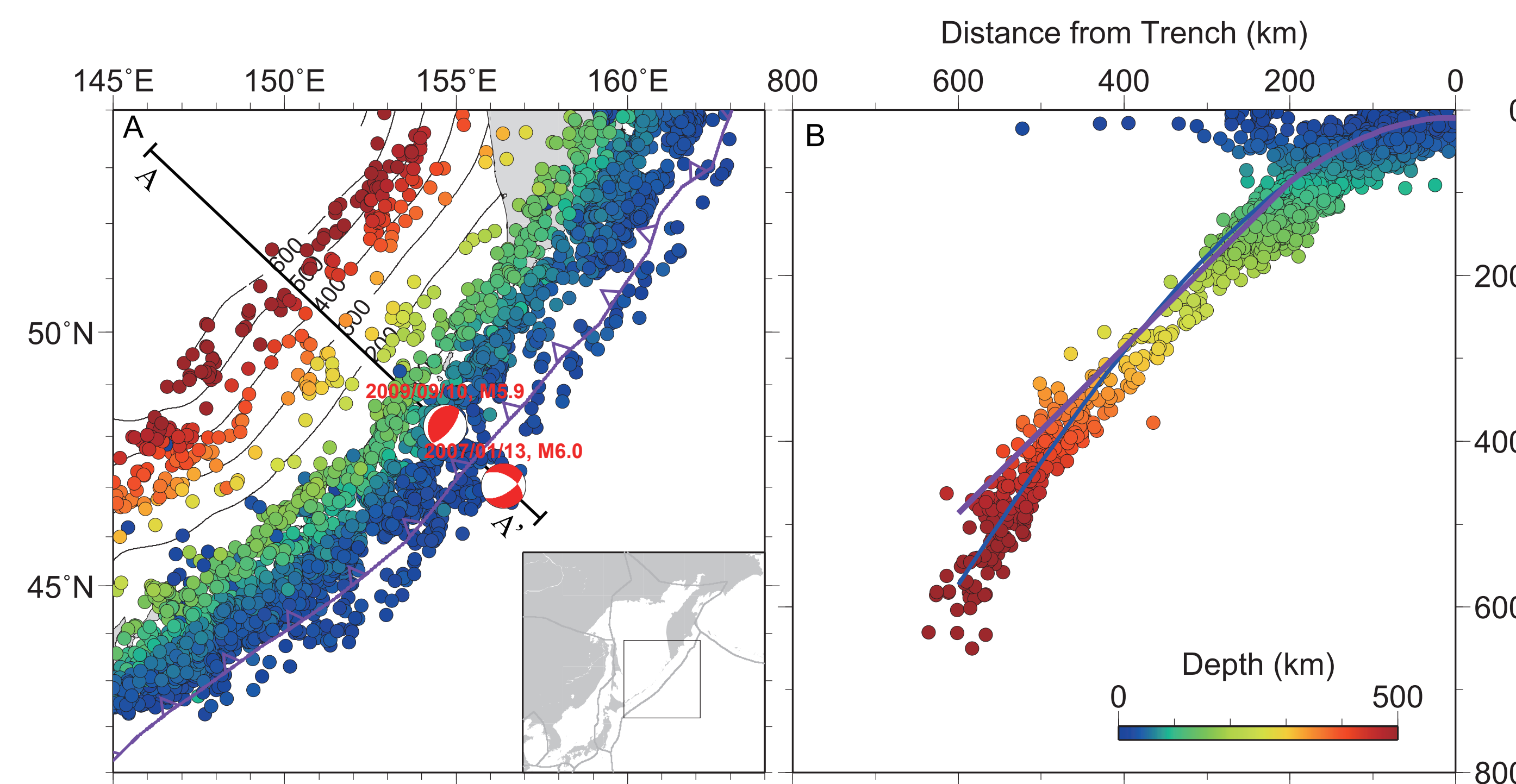


**Figure 2. Background seismicity and slab geometry.** (A) Map and relocated seismicity of the Kuril subduction zone. Box in the inset shows the location of our study area. The dots are the earthquakes in the EHB catalog from 1961 to 2008, colored by their depths. The slab contours are from Slab 1.0 (Hayes et al., 2010). The two red beachballs show the two earthquakes studied in this paper, one on each side of the trench (purple barbed line). AA' displays the location of cross-sections in Figure 3. (B) Plot of seismicity versus distance from trench and depth. The thick blue line is the slab geometry from the Slab 1.0, while the purple line is the modified geometry used here.

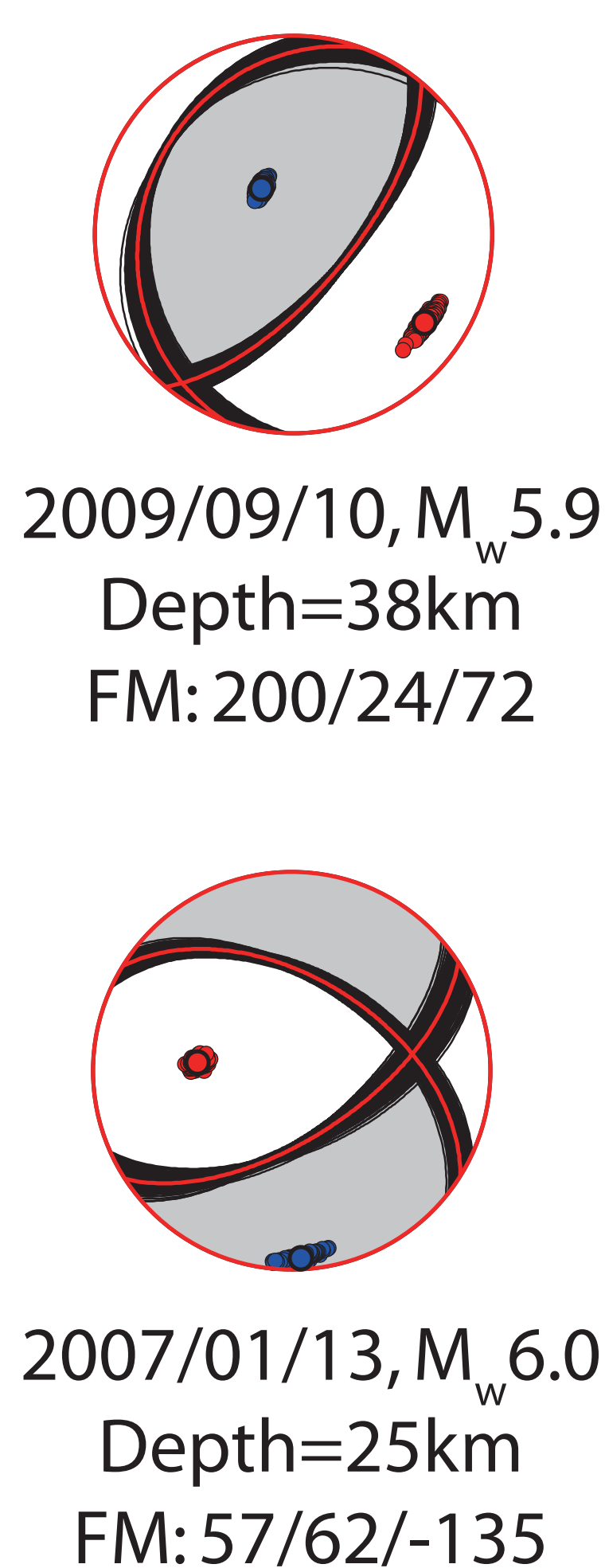


**Figure 3. Waveform observations and simulations** for the 2009/09/10 Mw5.9 interplate earthquake and the 2007/01/13 Mw6.0 outer-rise earthquake. (A) Distance record-sections of observed (left panel, black) and synthetic (right panel, red) seismograms for the 2009 interplate earthquake, aligned by the first P arrivals. (B) Similar to (A) but for the 2007 outer-rise earthquake. Figure S1 shows the comparisons of observed and synthetic full waveforms. (C) 2D finite-difference simulation of the 2009 interplate earthquake (red star) with a high-velocity slab (outlined by the white line). The inset shows the triangular velocity profile across the slab, with 5% perturbation in the slab center. Black lines display the P wave ray paths to teleseismic distances of 30°, 60° and 90°, respectively. (D) Similar to (C) but for the 2007 outer-rise earthquake.

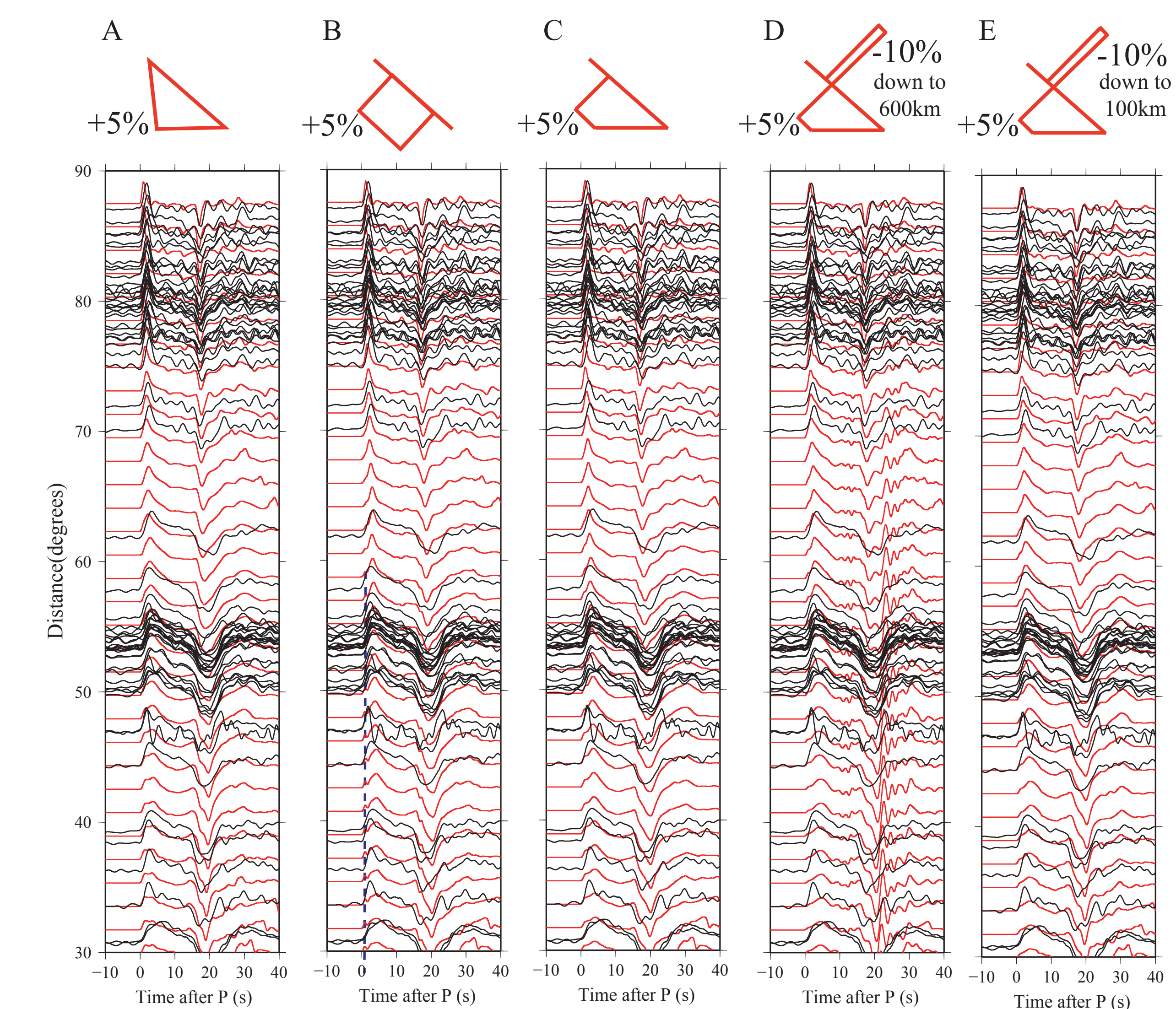


**Figure 4. Waveform sensitivities to slab sharpness.** For each panel, the observed seismograms are shown as black, and the synthetics using different velocity profiles across the slab (displayed on top) are in red. (A) has smooth edge on each side, (B) has sharp edges on both sides, (C) has sharp top but smooth bottom. (D) and (E) are modified from (C) with a low-velocity layer on top, to 600 km and 100 km, respectively.

## Conclusion and Future work

In this paper, we have studied the teleseismic P waveforms from two shallow earthquakes in the Kuril subduction zone to constrain the subducted slab structures. We observed strong distance-dependent waveform broadening and inverted for a high-velocity subducted slab with a triangular velocity profile. The maximum velocity perturbation in the slab core is 5%, significantly higher than most previous travel-time tomography models for this region.

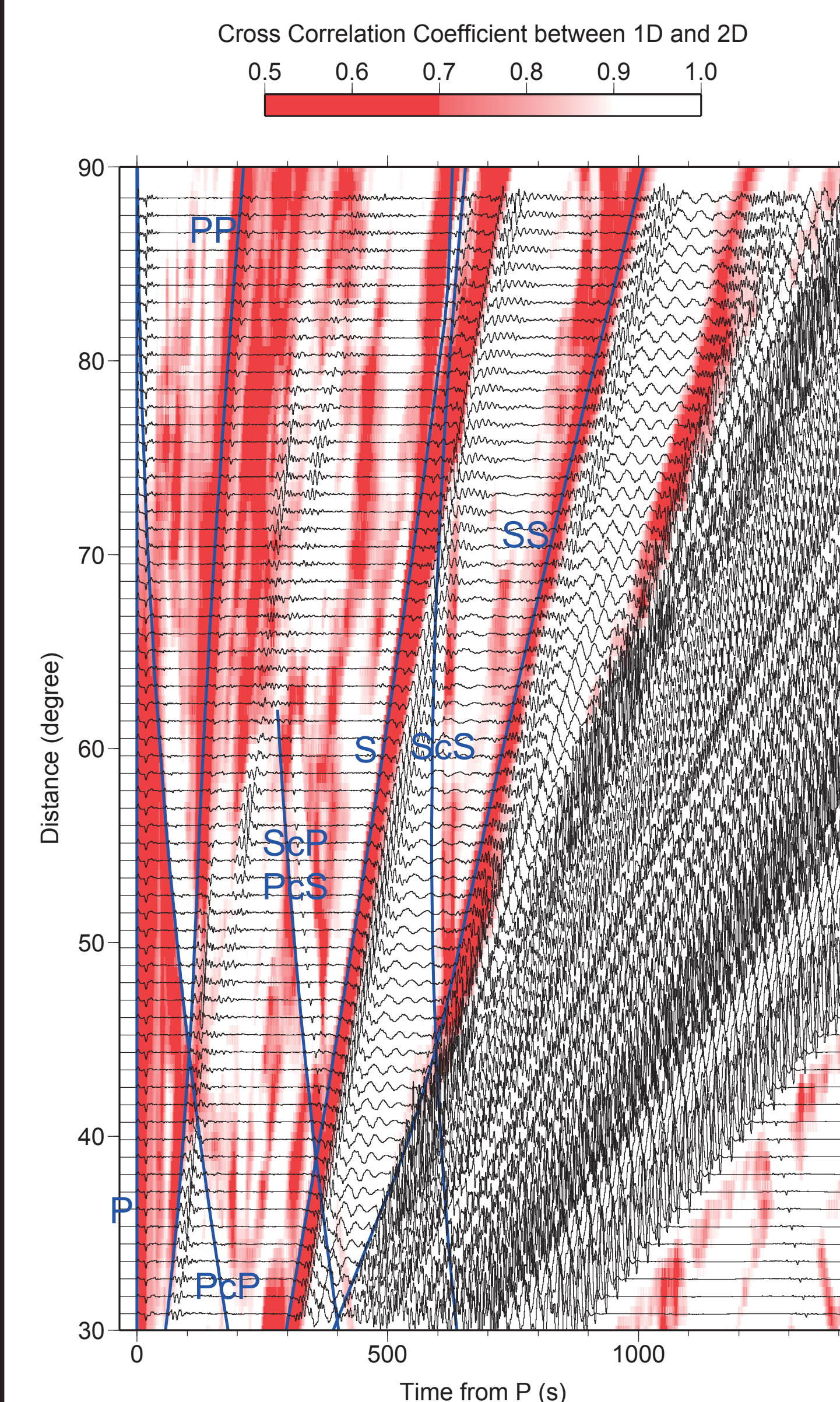


**Figure 5. slab-sensitive multibounce P and S waves.** Complete synthetic record section of the 2009 earthquake with the preferred slab model. The blue lines mark the major teleseismic body wave phases. The wave packages with largest amplitudes are the surface waves. To high-light the effect of the subducted slab, we compare the synthetic seismograms from models with/without the slab by cross-correlation. The background color shows the maximum cross-correlation coefficients allowing 5s shift. High cross-correlation (>0.9, white) means little waveform effect from slab, and low cross-correlation (<0.7, red color) highlights strongly distorted waveforms. Note that the surface waves with large amplitudes are not affected by the slab structure.